Nonlinear evolution of velocity fluctuations in a laminar boundary layer excited by free-stream vortical disturbances

Ricco, P.[1], Durbin, P.A.[2], Zaki, T.[2], and Wu, X.[1]
1 *Department of Mathematics, Imperial College, London, United Kingdom. and*
2 *Center for Turbulence Research, Stanford University, CA 94305, USA*

Ricco, P., Durbin, P. A., Zaki, T. & Wu, X. 2004 Nonlinear evolution of velocity fluctuations in a laminar boundary layer excited by free-stream vortical disturbances. In Proc. Summer Program 2004 , pp. 223–240. Centre for Turbulence Research.

The response of an incompressible laminar boundary layer to vortical disturbances in the free-stream is investigated. For sufficiently long-wavelength components, the unsteady boundary-*region* equations are employed at a streamwise location where the boundary-layer thickness becomes of the order of the inverse of the transverse fundamental wavenumber. The equations account for the transverse ellipticity and the pressure gradient induced by the displacement effect produced by the developing boundary layer. The free-stream turbulence is modeled by one vortical mode and the nonlinear generation of modes of higher frequency within the boundary layer is considered. This study confirms that low-frequency disturbances penetrate into the viscous region and induce laminar streamwise-elongated streaks, whereas high-frequency disturbances are confined in the outer edge layer. Results show that the streamwise and vertical wavenumbers have opposite effects on the penetration of modes into the boundary layer and that there is consistency between the linear boundary-region solution and the continuous spectrum of the Orr-Sommerfeld equation. Nonlinear effects are more intense for lower values of streamwise wavenumber for a fixed level of turbulence intensity.

I. INTRODUCTION

A. Background

The instability of laminar flows and transition to turbulence have interested researchers for over a century. Both the complexity of the physical mechanisms and the large range of applications have been the main factors for such research efforts. Since flows in engineering systems primarily exist in fully turbulent states, it is important to attain a sound understanding of the processes by which a laminar flow evolves to a turbulent regime. The ultimate engineering purpose is to design techniques for controlling these phenomena in order to reduce wall friction drag and noise, or to enhance heat transfer and mixing in combustion.

The first successful attempts to solve the problem of laminar instability in boundary layers date back to[45] and[40]. For the first time, the neutral curve of instability for the Blasius boundary layer was calculated and the unstable waves were thus named Tollmien-Schlichting (TS) waves, which were later first observed experimentally by[42]. They successfully reduced the free-stream turbulence to a very low level ($Tu = 0.01 - 0.03\%$) to suppress the undesired perturbations and detected the generation and evolution of TS waves excited by a vibrating ribbon. The TS waves were thus recognized as the key feature in laminar-turbulent flow transition. Laboratory observations by[9] and[44] had however showed that, when a laminar boundary layer was subjected to a high level of free-stream turbulence, low-frequency disturbances within the viscous region significantly amplified and distorted the flow. In this case the classical TS mechanism did not seem to play a significant role. This second type of disturbances found renewed interest with the investigations by[28] and[2]. They confirmed the findings by[9] and[44] and observed the existence of streak-like structures elongated in the streamwise direction. The transition process was not initiated by modal growth mechanisms, that is the TS viscous instability was *bypassed*. It thus appears that in the search for a sound understanding of instability and transition in wall-bounded flows it is necessary to determine when and how the TS process is excited as predicted by stability theory, and when the external level of

FIG. 1: Contour plot of streamwise velocity fluctuations in a plane parallel to the wall in the core of the boundary layer during bypass transition induced by free-stream turbulence. The flow is from left to right. DNS simulation by[?] .

perturbations is significant such that the growth of disturbances inside the viscous layer is not of the TS type. The problem is not trivial because it must additionally account for the different types of external disturbances which may excite the system.

It is known that the so-called *receptivity* process provides a mechanism capable of converting the wavelengths of the external disturbances into the wavelength proper of a TS wave. This may for example occur in the case of low-intensity free-stream turbulence ($Tu \sim 1\%$ or lower) interacting with wall-roughness and/or with other heterogeneities such as rapid changes in wall curvature and acoustic disturbances ([13];[14];[39];[16];[49]). On the contrary, in the cases of distortion of the free-stream flow and of higher free-stream turbulence levels, the route to wall-bounded turbulence does not follow the classical TS wave mechanism.[50] showed that moderate free-stream turbulence may induce substantially excessive growth rates so that the modified amplification of TS waves is higher than in the case of the undisturbed Blasius boundary layer. They also argued that, when the distortion exceeds a certain threshold, the mean profile shows a near-wall inflection point which drives the system to inviscid instability. For even higher free-stream turbulence levels ($Tu > 2-3\%$), bypass transition appears to take effect, which still remains mysterious. The boundary layer acts like a filter, allowing low-frequency perturbations to penetrate into the boundary layer, convect downstream and intensify ([38];[35];[43];[18];[17];[19];[1]). As outlined by[24], the laminar boundary layer initially undergoes a phase during which the skin-friction is only slightly higher than in the purely laminar regime. Laminar streamwise-elongated streaks, known as breathing modes or "Klebanoff modes" ([26];[48]) dominate the core of the viscous region in this first stage of external excitation. Although these structures are called "modes", they are not modes in the strict mathematical sense, namely they are not solutions to an eigenvalue problem. The next stage of transition is the generation of small scales of motion which eventually lead to the formation of turbulent spots. The turbulent boundary layer is then formed by the merging of the spots. Figure 1 shows a top view of the downstream evolution of streamwise velocity fluctuations inside the boundary layer when excited by free-stream turbulence. The formation of the laminar streaks (left), their instability and breakdown to turbulent spots and the merging to fully-developed turbulence (right) are clearly pictured.

Recent effort has been directed to providing a mathematical description of the linear growth of the laminar streaks. It has been found that in a laminar wall-bounded flow, three-dimensional disturbances with very long or infinite streamwise wavelength may undergo transient temporal algebraic growth to form streaks ([10];[29];[22];[21];[4];[46];[37]). More recently, it was shown that three-dimensional disturbances of similar form may exhibit substantial spatially-transient downstream growth in a flat-plate boundary layer ([32];[33];[6];[47];[53]). All these works revealed an important characteristic concerning the development of streamwise vortices which are already present within the undary layer. Even the predicted profiles of the perturbation agree fairly well with experimental measurements. However, these works did not explain the key process of how these perturbations are generated by free-stream disturbances, and so these theories do not fully describe the bypass transition induced by external turbulence.

We argue that any research attempt aimed at understanding bypass transition must explicitly account for the forcing of external disturbances, which appear to be the predominant cause for this unique phenomenon. The model must thus be an inhomogeneous problem with non-zero boundary

conditions at the edge of the boundary layer in order to synthesize the effects of the interaction of the viscous layer with external perturbations such as free-stream turbulence.

Steps in this direction have been taken by[30] (denoted as LWG), and by the DNS study by[24] and[?] . In these last two works, the free-stream turbulence is expanded in continuous spectrum modes. The penetration depth of these modes provides a characterization of the ability of the external disturbance to generate amplifying disturbances inside the boundary layer. In contrast to the studies of algebraic growth, where the boundary-layer excitation is modeled as a homogeneous problem, they investigated the entrainment of free-stream velocity disturbances into a flat-plate boundary layer.

B. Organization of the paper

Nonlinear unsteady boundary-region solution

The mathematical formulation first hinges on the boundary-layer equations which provide a valid description of the response relatively close to the leading edge. The elliptic boundary-region equations, however, must be invoked farther downstream where the boundary-layer thickness grows to a size comparable with a length scale representative of the transverse vortical motion. The linear variant of these equations (LUBR) was solved by LWG. The nonlinear extension is not trivial, and represents the major challenge of the present analysis. The equations of continuity, x-, y- and z-momentum for the disturbances are solved by employing a second-order backward finite-difference scheme. The solution of this system requires an initial field, as well as upstream and free-stream boundary conditions.

Mean laminar steady flow

The boundary-layer equations for the mean laminar flow are first solved to obtain the background flow on which the perturbations evolve. The equations are cast into the usual nondimensional form which employs the similarity variable η and gives the well-known Blasius solution ([41]). The system is solved through a second-order finite-difference scheme which employs Newton's method ([7]).

Inviscid free-stream flow and outer boundary conditions

The mean inviscid flow is affected at leading order by the displacement effect induced by the viscous region. The free-stream solution is matched with the solution of the large-η form of the equations to find the $\eta \to \infty$ boundary conditions.

Initial condition

These profiles are needed in order to initiate the boundary-region calculation. They are obtained by means of a composite solution, constructed from the large-η solution and a power series valid for $\eta = \mathcal{O}(1)$, and by using the additive rule.

C. Objective

The objective of the present analysis is twofold. Our main focus is to extend the calculations of LWG, restricted to the linear evolution of very small perturbations, to the nonlinear interaction of fluctuations within the boundary layer forced by one free-stream mode.

Although LWG showed that the linear unsteady boundary-region equations describe well the behavior of low-amplitude fluctuations relatively close to the leading edge, nonlinearity must be necessarily accounted for as the magnitude of disturbances grows downstream. As LWG and[52] point out, its effects are likely to be the enhancement of transverse-length-scale components and the generation of high-frequency disturbances. In another paper of theirs,[31] report preliminary results for the nonlinear evolution of the peak level of the transverse-averaged r.m.s. component of the streamwise velocity as a function of the boundary-layer thickness. The solution was obtained by solving the *steady* boundary-region equations with one free-stream mode. The nonlinear solution

agrees well with the linear one for short streamwise distances, while the nonlinear trend is lower than the linear one farther downstream.

The second objective is to study the effect of the parameters of the free-stream modes on the penetration of disturbances into the boundary layer. The frequencies of the modes in the streamwise and wall-normal directions are varied independently and the linear boundary-region equations are solved. The results are compared with the penetration of the modes given by the Orr-Sommerfeld equations. The comparison of the two different approaches is motivated by the work of[24], where the continuous spectrum of the OS modes is used to synthesize the inflow condition for a DNS of bypass transition.

II. PROBLEM FORMULATION: SCALING AND EQUATIONS OF MOTION

The two-dimensional flow of uniform velocity U_∞ past an infinitely-thin flat plate on which homogeneous three-dimensional, statistically-stationary turbulent velocity fluctuations are superposed is considered. These perturbations are of the convected "gust" type, i.e. they passively convect with the mean flow. The mean velocity of the oncoming flow is significantly smaller than the speed of sound so that the flow can be considered incompressible. The * symbol indicates dimensional quantities. The Cartesian coordinate system is represented by the vector $\mathbf{x} = x\hat{\mathbf{i}}+y\hat{\mathbf{j}}+z\hat{\mathbf{k}} = x_1\hat{\mathbf{i}}+x_2\hat{\mathbf{j}}+x_3\hat{\mathbf{k}}$, which defines the streamwise, wall-normal and transverse directions, respectively. In LWG, these coordinates and all the other lengths are nondimensionalized by the transverse integral scale of turbulence Λ, which is defined as follows:

$$\Lambda = \Lambda(x^*, y^*) = \int_0^\infty R_{ww}(x^*, y^*, \tau)\mathrm{d}\tau,$$

where the correlation of the transverse velocity component is

$$R_{ww}(x^*, y^*, \tau) = \frac{\overline{w_\infty(x^*, y^*, z^*+\tau, t^*)w_\infty(x^*, y^*, z^*, t^*)}}{\overline{(w_\infty(x^*, y^*, z^*, t^*))^2}}.$$

The overbar indicates time-averaged quantities and it is considered that $x^* \to -\infty$ and $y^* \to \infty$ so that Λ is constant. For our case of one mode in the free-stream, it occurs that:

$$R_{ww} = \cos(k_3^*\tau),$$

so that Λ is not defined. We thus choose to scale all the lengths by the inverse of the transverse fundamental wavenumber k_3^*. For clarity, we still call this reference length $\Lambda = 1/k_3^*$, hence $k_3 = 1.0$. The velocity quantities are made dimensionless by U_∞. The pressure p^* is normalized by ρU_∞^2 and the time t^* by Λ/U_∞.

Due to the hypothesis of homogeneity and stationariety of the statistical quantities, such fluctuations are mathematically represented as a superposition of sinusoidal disturbances:

$$\mathbf{u} - \hat{\mathbf{i}} = \varepsilon\mathbf{u}_\infty(x-t, y, z) = \varepsilon\hat{\mathbf{u}}^\infty e^{i(\mathbf{k}\cdot\mathbf{x}-k_1 t)} + c.c., \tag{1}$$

where $\hat{\mathbf{u}}^\infty = \{\hat{u}_1^\infty, \hat{u}_2^\infty, \hat{u}_3^\infty\}$ and $\mathbf{k} = \{k_1, k_2, k_3\}$ are real vectors and $\hat{u}_{1,2,3}^\infty = \mathcal{O}(1)$. From the incompressibility condition, it follows that:

$$\nabla\cdot\mathbf{u}_\infty = 0, \text{ namely } \hat{\mathbf{u}}^\infty\cdot\mathbf{k} = 0. \tag{2}$$

Differently from the linear analysis by LWG where the turbulent Reynolds number

$$r_t = \varepsilon R_\Lambda << 1,$$

we have $r_t = \mathcal{O}(1)$, where

$$R_\Lambda = \frac{U_\infty \Lambda}{\nu}$$

is the Reynolds number based on Λ and on the kinematic viscosity of the fluid ν. We also assume to work in the high-Reynolds-number regime, i.e. $R_\Lambda >> 1$. It has been shown by[15] that, as $\varepsilon \to 0$ while r_t is kept at $\mathcal{O}(1)$, the flow domain can be divided into four distinct asymptotic regions, shown in figure 2. Here is a brief description of the regions:

Region I: This region of dimensions $\mathcal{O}(\Lambda)$ in the vertical and streamwise directions includes the inviscid linear flow approaching the leading edge of the plate. In this region, the disturbances are treated as small perturbations of the oncoming uniform flow. The behavior of the solution in the very proximity of the leading edge is not considered. Instead, the analysis concentrates on the downstream asymptotic evolution of the disturbances at a large distance from the edge, allowing the derivatives with respect to the streamwise direction to be neglected.

Region II: This region is located under Region I and it comprises the viscous flow as it develops from the leading edge of the plate. The disturbances are governed by the linearized unsteady boundary-layer equations (LUBL) ([12]; LWG). The solution eventually becomes invalid when the boundary-layer thickness δ^* becomes of the order of Λ. Since δ^* evolves as:

$$\delta^* = \Lambda\delta = \mathcal{O}(x^* R^{-1/2}),$$

where $R = x^* U_\infty/\nu$, setting $\delta^* = \mathcal{O}(\Lambda)$ implies that the boundary-layer approximation becomes invalid at a downstream location where $x^* = \mathcal{O}(\Lambda R_\Lambda)$, namely where

$$x/R_\Lambda = \mathcal{O}(1).$$

The flow then becomes fully three-dimensional and the ellipticity in the transverse direction must be considered. The initial condition for LUBL is used to construct the initial condition for the flow in Region III.

Region III: The flow in this region is mathematically described by the unsteady boundary-region equations ([25]), which are a simplified version of the full Navier–Stokes equations, obtained by discarding the streamwise derivatives in the viscous and pressure-gradient terms. These equations are different from the ones of LWG because the nonlinear terms are not neglected any longer.

Region IV: This region describes the outer inviscid flow above Region III and the solution is influenced at leading order by the displacement effect due to the increased thickness of the viscous layer. The flow should generally be considered nonlinear since turbulence experiences equilibrium decay in this region. However, as argued by LWG, the flow can be regarded as linear over a range of streamwise distances if the turbulent Reynolds number $r_t << 1$ and the flow behaves locally as a convected perturbation gust of the type of Region I. This happens when the distance $x_L << 1/\varepsilon = R_\Lambda/r_t$. Following the study by LWG, the stationary and homogeneous turbulence $\varepsilon \mathbf{u}_\infty$ is specified at a distance $-x_L^\dagger$ upstream of the leading edge where:

$$1 << -x_L^\dagger << R_\Lambda. \tag{3}$$

The boundary condition (1) can thus be applied independently of the mean flow. Despite the fact that the linear flow in the free-stream suitably provides the outer boundary conditions for the nonlinear boundary-region equations, the effects of nonlinearity in the free-stream deserve further analysis. Additional comments on this issue can be found in section II B.

The flow in Region I is inviscid and treated as a flow of uniform velocity to which gust-like velocity perturbations are superposed. The inviscid perturbations can be determined by rapid distortion theory ([23];[11]), which describes the interaction of a gust-like disturbance with a body of arbitrary shape, in our case an infinitely-thin flat plate. The inviscid perturbation $\{u_{1,w}, u_{2,w}, u_{3,w}\}$ at the surface of the plate gives the outer boundary conditions for the viscous flow in Region II:

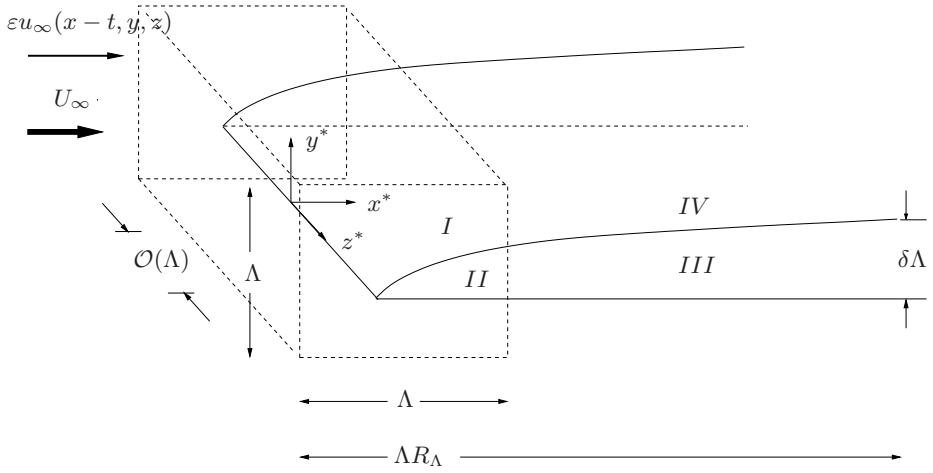

FIG. 2: Flow field domain representation.

$$u_{1,w} = \hat{u}_1^\infty + \frac{ik_1}{\gamma}\hat{u}_2^\infty, \tag{4}$$

$$u_{3,w} = \hat{u}_3^\infty + \frac{ik_3}{\gamma}\hat{u}_2^\infty, \gamma = \sqrt{k_1^2 + k_3^2}, \tag{5}$$

where the first terms on the right-hand side are the components of the unperturbed gust disturbance. The second terms represent the influence of the underlying flat surface and are related to the potential flow induced by the gust interacting with the plate. These large-η conditions are employed to obtain the initial profiles for the flow in Region II, which, in turn, are used to determine the boundary conditions for Region III. The complete analysis can be found in LWG.

A. The unsteady nonlinear boundary-region equations

For a single Fourier component of the disturbance, the physical solution in the viscous region can be expressed as:

$$\{u,v,w,p\} = \{F', \left(\frac{1}{2xR_\Lambda}\right)^{1/2}(\eta F' - F), 0, -\frac{1}{2}\} \; +$$

$$+ \quad \varepsilon\{\overline{u}_0(\overline{x},\eta,z,t), \left(\frac{2\overline{x}k_1}{R_\Lambda}\right)^{1/2}\overline{v}_0(\overline{x},\eta,z,t), \overline{w}_0(\overline{x},\eta,z,t), \overline{p}_0(\overline{x},\eta,z,t)\}, \tag{6}$$

where:

$$\eta = y\left(\frac{R_\Lambda}{2x}\right)^{1/2},$$

and $\overline{x} = k_1 x$. $F = F(\eta)$ is the Blasius function, solution of:

$$F''' + FF'' = 0,$$

with $F(0) = 0$, $F'(0) = 0$ and $F \to \overline{\eta} = \eta - \beta$ ($\beta = 1.2168$) as $\eta \to \infty$. As in LWG and[20], the perturbation solution is expressed as the sum of a two-dimensional part $\{\overline{u}^{(0)}, \overline{v}^{(0)}, 0, \overline{p}^{(0)}\}$ and a three-dimensional part, as follows:

$$\overline{u}_0 = \overline{u}^{(0)} + \sum_{m,n=-\infty}^{+\infty} \hat{u}_{m,n} e^{ink_3 z - imk_1 t}, \tag{7}$$

$$\overline{v}_0 = \overline{v}^{(0)} + \sum_{m,n=-\infty}^{+\infty} \hat{v}_{m,n} e^{ink_3 z - imk_1 t}, \tag{8}$$

$$\overline{w}_0 = \sum_{m,n=-\infty}^{+\infty} \hat{w}_{m,n} e^{ink_3 z - imk_1 t}, \tag{9}$$

$$\overline{p}_0 = \overline{p}^{(0)} + \sum_{m,n=-\infty}^{+\infty} \hat{p}_{m,n} e^{ink_3 z - imk_1 t}. \tag{10}$$

The equations of motion are then obtained by inserting expressions (7)-(10) into the nonlinear boundary-region equations and by retaining the three-dimensional components only:

Continuity equation

$$\frac{\partial \hat{u}_{m,n}}{\partial \overline{x}} - \frac{\eta}{2\overline{x}} \frac{\partial \hat{u}_{m,n}}{\partial \eta} + \frac{\partial \hat{v}_{m,n}}{\partial \eta} + n\Omega \hat{w}_{m,n} = 0; \tag{11}$$

x-Momentum equation

$$\left(-im - \frac{\eta F''}{2\overline{x}} + n^2\kappa^2\right) \hat{u}_{m,n} + F' \frac{\partial \hat{u}_{m,n}}{\partial \overline{x}} - \frac{F}{2\overline{x}} \frac{\partial \hat{u}_{m,n}}{\partial \eta} - \frac{1}{2\overline{x}} \frac{\partial^2 \hat{u}_{m,n}}{\partial \eta^2} +$$

$$+ F'' \hat{v}_{m,n} = -\varepsilon \widehat{\frac{\partial (u_{\mathrm{R}} u_{\mathrm{R}})}{\partial \overline{x}}}|_{m,n} + \frac{\varepsilon\eta}{2\overline{x}} \widehat{\frac{\partial (u_{\mathrm{R}} u_{\mathrm{R}})}{\partial \eta}}|_{m,n} +$$

$$- \varepsilon \widehat{\frac{\partial (u_{\mathrm{R}} v_{\mathrm{R}})}{\partial \eta}}|_{m,n} - \varepsilon n \Omega \widehat{u_{\mathrm{R}} w_{\mathrm{R}}}|_{m,n}; \tag{12}$$

y-Momentum equation

$$\frac{1}{4\overline{x}^2} \left(F - \eta F' - \eta^2 F''\right) \hat{u}_{m,n} + \left(-im + \frac{F'}{2\overline{x}} + \frac{\eta F''}{2\overline{x}} + n^2\kappa^2\right) \hat{v}_{m,n} +$$

$$+ F' \frac{\partial \hat{v}_{m,n}}{\partial \overline{x}} - \frac{F}{2\overline{x}} \frac{\partial \hat{v}_{m,n}}{\partial \eta} - \frac{1}{2\overline{x}} \frac{\partial^2 \hat{v}_{m,n}}{\partial \eta^2} + \frac{R_\Lambda}{2\overline{x} k_1} \frac{\partial \hat{p}_{m,n}}{\partial \eta}$$

$$= -\frac{\varepsilon}{2\overline{x}}\widehat{u_{\rm R}v_{\rm R}}|_{m,n} - \varepsilon\widehat{\frac{\partial(u_{\rm R}v_{\rm R})}{\partial\overline{x}}}|_{m,n} +$$

$$+ \frac{\varepsilon\eta}{2\overline{x}}\widehat{\frac{\partial(u_{\rm R}v_{\rm R})}{\partial\eta}}|_{m,n} - \varepsilon\widehat{\frac{\partial(v_{\rm R}v_{\rm R})}{\partial\eta}}|_{m,n} - \varepsilon n\Omega\widehat{v_{\rm R}w_{\rm R}}|_{m,n}; \tag{13}$$

z-Momentum equation

$$(-im + n^2\kappa^2)\hat{w}_{m,n} + F'\frac{\partial\hat{w}_{m,n}}{\partial\overline{x}} - \frac{F}{2\overline{x}}\frac{\partial\hat{w}_{m,n}}{\partial\eta} - \frac{1}{2\overline{x}}\frac{\partial^2\hat{w}_{m,n}}{\partial\eta^2}$$

$$+n\Omega\hat{p}_{m,n} = -\varepsilon\widehat{\frac{\partial(u_{\rm R}w_{\rm R})}{\partial\overline{x}}}|_{m,n} + \frac{\varepsilon\eta}{2\overline{x}}\widehat{\frac{\partial(u_{\rm R}w_{\rm R})}{\partial\eta}}|_{m,n}$$

$$- \varepsilon\widehat{\frac{\partial(v_{\rm R}w_{\rm R})}{\partial\eta}}|_{m,n} - \varepsilon n\Omega\widehat{w_{\rm R}w_{\rm R}}|_{m,n}, \tag{14}$$

where

$$\kappa \equiv \frac{k_3}{(k_1 R_\Lambda)^{1/2}} = \mathcal{O}(1), \tag{15}$$

and $\Omega = ik_3/k_1$. The $\widehat{\ }$ symbol on the nonlinear terms indicates the Fourier transform operation and the subscript R denotes the three-dimensional component of velocity in equations (7)-(10). The equations are parabolic in the $\overline{x}$ direction and elliptic in the z direction. A second-order backward finite-difference scheme is employed to march in $\overline{x}$ and the block tri-diagonal system is solved with a standard block-elimination algorithm. The pressure component is computed on a grid staggered in the η direction with respect to the grid of the velocity components. The nonlinear terms are evaluated explicitly using the pseudospectral method, namely the velocity quantities at the previous $\overline{x}$ location are transformed back to the physical space to perform the product operations and are subsequently Fourier transformed again to the spectral space. This is a standard procedure for similar flow simulations in order to avoid the computationally expensive convolution operations ([27]). Dealiasing is performed by expanding the number of collocation points by a factor of (at least) 3/2 before going from the spectral to the physical space ([5],[34],[36]). This operation avoids the spurious energy cascade from the unresolved high-frequency modes into the resolved low-frequency ones and it is found to be essential for the stability of the numerical results when the effect of nonlinearity is significant. An odd number of modes $N_t = N_z = 9$ is employed and is sufficient for capturing the nonlinear effects. The domain extends to $\eta = 20$ and 500 grid points are used in this direction. The typical step size in the marching direction is $\Delta\overline{x} = 0.005$.

B. Initial and boundary conditions

The initial condition is the same as in LWG and corresponds to the mode $(m, n) = (1, 1)$. Null initial velocity and pressure profiles are specified for all the other modes. The initial conditions are then:

$$\hat{u}_{1,1} \to \Omega u_{3,w}\left(2\overline{x}U_0 + (2\overline{x})^{3/2}U_1\right), \tag{16}$$

$$\hat{v}_{1,1} \to \Omega u_{3,w} \Bigg((V_0 + (2\overline{x})^{1/2} V_1 + \frac{i}{(\kappa_2 - i|\kappa|)(2\overline{x})^{1/2}} \Big(e^{i\kappa_2 (2\overline{x})^{1/2}\overline{\eta} - (\kappa^2 + \kappa_2^2)\overline{x}} -$$

$$+ e^{-|\kappa|(2\overline{x})^{1/2}\overline{\eta}} \Big) - \left(\frac{3}{4}\beta - \frac{1}{2} g_1 |\kappa| (2\overline{x})^{1/2} \right) e^{-|\kappa|(2\overline{x})^{1/2}\overline{\eta}} +$$

$$+ \overline{\eta} + \frac{3}{4}\beta - (2\overline{x})^{1/2} \left(-\frac{i}{2}(\kappa_2 + i|\kappa|)(\overline{\eta}^2 + 1) + \frac{3}{4}\beta|\kappa|\overline{\eta} + \frac{1}{2}|\kappa| g_1 \right) \Bigg), \tag{17}$$

$$\hat{w}_{1,1} \to u_{3,w} \Bigg(W_0 + (2\overline{x})^{1/2} W_1 + \frac{1}{(\kappa_2 - i|\kappa|)} \Big(\kappa_2 e^{i\kappa_2 (2\overline{x})^{1/2}\overline{\eta} - (\kappa^2 + \kappa_2^2)\overline{x}} +$$

$$- i|\kappa| e^{-|\kappa|(2\overline{x})^{1/2}\overline{\eta}} \Big) - \frac{3}{4}\beta|\kappa|(2\overline{x})^{1/2} e^{-|\kappa|(2\overline{x})^{1/2}\overline{\eta}} - 1 +$$

$$- (2\overline{x})^{1/2} \left(i(\kappa_2 + i|\kappa|)\overline{\eta} - \frac{3}{4}\beta|\kappa| \right) \Bigg), \tag{18}$$

$$\hat{p}_{1,1} \to \frac{ik_3}{R_\Lambda} u_{3,w} \left(P_1 + \left(g_1 - \frac{3}{4} \frac{\beta}{|\kappa|(2\overline{x})^{1/2}} \right) e^{-|\kappa|(2\overline{x})^{1/2}\overline{\eta}} - g_1 - \frac{3}{4}\beta\overline{\eta} \right), \tag{19}$$

where the functions U_0, V_0, W_0 and U_1, V_1, W_1, P_1 are solutions to two linear systems given in Appendix B, pag. 199 of LWG. It is also given that

$$\kappa_2 \equiv \frac{k_2}{(k_1 R_\Lambda)^{1/2}}, \tag{20}$$

and the condition $k_1 << k_2, k_3$ applies. The complex constant g_1 is also given in Appendix B, pag. 200 of LWG and is obtained by matching the large-η solution of the linear boundary-region equations with the initial condition for the linear boundary-layer equations. The no-slip boundary condition is applied at the wall for the velocity components of all the modes. Thanks to the staggered grid, no boundary condition for the pressure fluctuation is required at the wall. The boundary conditions as $\eta \to \infty$ for the forcing mode $(m, n) = (1, 1)$ capture the turbulent viscous decay in the free-stream and are of the mixed type:

$$\hat{u}_{1,1} \to 0, \tag{21}$$

$$\frac{\partial \hat{v}_{1,1}}{\partial \eta} + |\kappa|(2\overline{x})^{1/2} \hat{v}_{1,1} \to -\Omega u_{3,w} e^{i(\overline{x} + \kappa_2 (2\overline{x})^{1/2}\overline{\eta})} e^{-(\kappa^2 + \kappa_2^2)\overline{x}}, \tag{22}$$

$$\frac{\partial \hat{w}_{1,1}}{\partial \eta} + |\kappa|(2\overline{x})^{1/2} \hat{w}_{1,1} \to i u_{3,w} \kappa_2 (2\overline{x})^{1/2} e^{i(\overline{x} + \kappa_2 (2\overline{x})^{1/2}\overline{\eta})} e^{-(\kappa^2 + \kappa_2^2)\overline{x}}, \tag{23}$$

$$\frac{\partial \hat{p}_{1,1}}{\partial \eta} + |\kappa|(2\overline{x})^{1/2} \hat{p}_{1,1} \to 0. \tag{24}$$

Case	k_1	k_2	k_3	$\overline{x}$
1	0.00053	-0.667	1.0	0.1
2	0.0011	-0.667	1.0	0.2
3	0.011	-0.667	1.0	2.0
4	0.063	-0.667	1.0	12.0
5	0.212	-0.667	1.0	40.0

TABLE I: Parameters for the mode comparison at $R_\Lambda = 212$ depicted in figures 3 and 5 for the LUBR and the OS solutions, respectively.

Case	k_1	k_2	k_3	$\overline{x}$
a	0.1333	-1.0	1.0	32.0
b	0.1333	-1.167	1.0	32.0
c	0.1333	-1.333	1.0	32.0
d	0.1333	-1.5	1.0	32.0

TABLE II: Parameters for the mode comparison at $R_\Lambda = 167$ depicted in figures 4 and 6 for the LUBR and the OS solutions, respectively.

For the other modes generated by nonlinearity within the viscous region, the boundary conditions as $\eta \to \infty$ are:

$$\hat{u}_{m,n} = \hat{v}_{m,n} = \hat{w}_{m,n} = \hat{p}_{m,n} = 0, \text{for } (m,n) \neq (1,1). \tag{25}$$

Small and bounded oscillations appear in the profiles of these velocity components at short downstream distances and eventually die away as $\overline{x}$ increases. These oscillations are probably due to the null initial profiles and to the fact that these large-η boundary conditions indeed only represent the asymptotic behavior as $\overline{x} \to \infty$. It must be also remarked that nonlinear effects might be present in the free-stream. This issue was already pointed out by LWG. Nonlinear terms should then be retained in the free-stream equations and in the large-η boundary-region equations, which are both employed to find the outer boundary conditions. We observe that, albeit generated within the boundary layer, the v, w and p component of the nonlinearly-excited modes with $(m,n) > (1,1)$ extend well beyond the limit of the boundary layer at $\eta \approx 3.5$. For the present status of the analysis we have tried to overcome this problem by employing a very large domain extending to $\eta = 20$.

III. RESULTS

A. Penetration of modes into the boundary layer

The values of the wavenumbers k_1 and k_2 are independently varied to study the penetration of the free-stream modes into the boundary layer and are given in tables I and II. We analyze the shape of the real component of the three-dimensional linear boundary-layer solution $\{\overline{u}_R^+, \overline{v}_R^+, \overline{w}_R^+\}$ for $t = 0$ and $z = 0$ at fixed downstream location x. The superscript $+$ indicates quantities scaled by the maximum free-stream value. The OS and LUBR equations are employed for comparison. Lower values of k_1 generate a more penetrating $\overline{v}_R^+$ (figures 3 and 5) and $\overline{u}_R^+$ components (not shown). The same effect is detected on the transverse component of velocity, but it is less intense than on the other components. The present results underline the importance of k_1 on the penetration of the modes into the viscous region. Similarly to what[24] and LWG observed, the boundary layer acts as a low-pass filter, so that high-frequency fluctuations are sheltered and do not diffuse toward the wall.

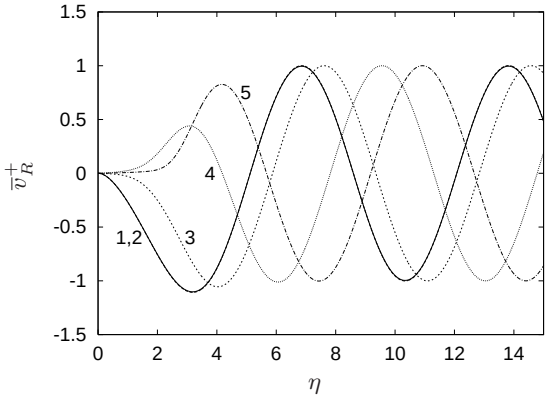

FIG. 3: Instantaneous profiles of vertical velocity component for different values of k_1 - OS solution - $R_\Lambda = 212$.

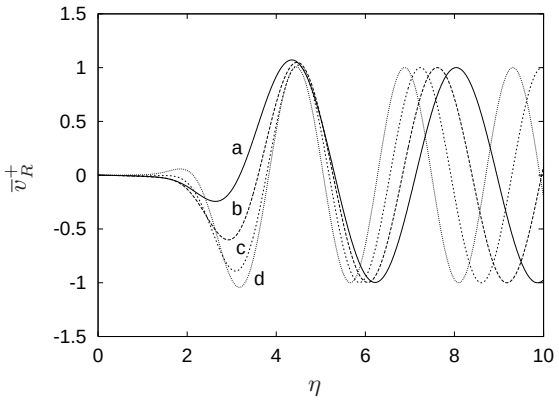

FIG. 4: Instantaneous profiles of vertical velocity component for different values of k_2 - OS solution - $R_\Lambda = 167$.

Figures 4 and 6 show that k_2 has the opposite effect of k_1: lower values of k_2 give less penetration of the modes into the boundary layer. The OS equations give qualitatively similar results to the LUBR equations, thus indicating that the non-parallel effects do not play a major role in the penetration of modes into the boundary layer. The non-parallel effects may however become significant during the downstream evolution for the *lift-up* phenomenon detected in the DNS simulations by[24], although nonlinearity probably plays a more critical role.

B. Nonlinear evolution of disturbances in the boundary layer

In order to quantify the effect of the external forcing within the boundary layer, we study the $\overline{x}$ evolution of the maximum value along η of the r.m.s of the fluctuating streamwise velocity component. The r.m.s. is defined as:

$$\overline{u}_{RMS} = \varepsilon \left(\sum_{m=-(N_t-1)/2}^{(N_t-1)/2} \sum_{n=-(N_z-1)/2}^{(N_z-1)/2} |\hat{u}_{m,n}|^2 \right)^{1/2}, (m,n) \neq (0,0).$$

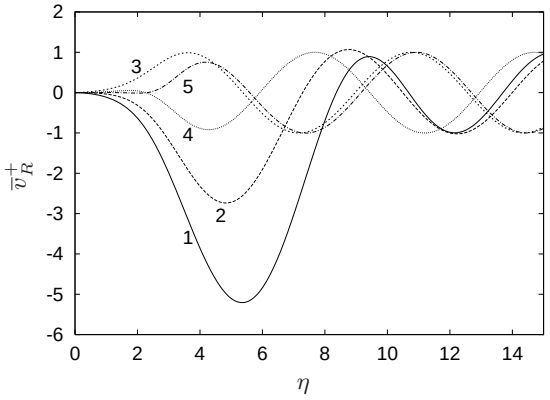

FIG. 5: Instantaneous profiles of vertical velocity component for different values of k_1 - LUBR solution - $R_\Lambda = 212$.

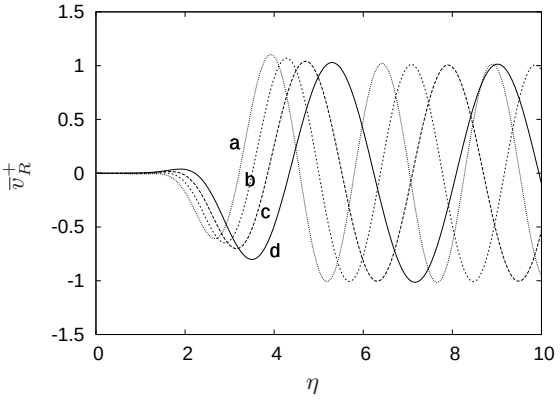

FIG. 6: Instantaneous profiles of vertical velocity component for different values of k_2 - LUBR solution - $R_\Lambda = 167$.

The peak of this quantity is then compared with the peak of the r.m.s. of the linear solution, namely:

$$\overline{u}_{RMS} = \varepsilon\sqrt{2}|\Omega u_{3,w}\overline{u}|,$$

where $\overline{u}$ is the same as in LWG.

Nonlinearity has a stabilizing influence on the evolution of the r.m.s signal. The linear trend coincides with the nonlinear one at short downstream distances, and the effect becomes gradually more important as the flow develops downstream until it saturates. As shown in figures 7 and 8, lower values of streamwise frequencies k_1 and higher values of free-stream Tu amplify this effect, with a more marked influence of the latter. This is in agreement with the observation that low frequency modes are the most penetrating ones.

LWG partly attributed the discrepancy between their high-frequency linear results (LWG Figure 10 - page 192) and the experimental data by Kendall (unpublished) to nonlinear effects. In our study, these effects are captured, but do not explain the divergence in LWG's results at high frequency because the low-frequency fluctuations are the ones which are most influenced by nonlinearity. It should be noted, however, that high-frequency disturbances are the ones most likely to be affected by streamwise ellipticity effects, neglected both in LWG's work and in ours. Also, LWG's solution is

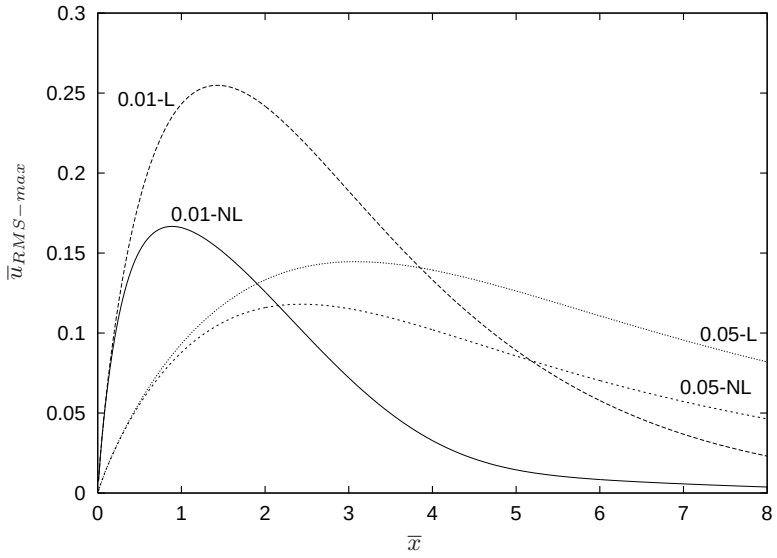

FIG. 7: Effect of variation of streamwise wavenumber k_1 on the maximum r.m.s. of the streamwise velocity for $\varepsilon\hat{u}^{\infty}_{1,2,3} = 0.015$, $k_2 = -k_3 = -1.0$ and $R_\Lambda = 400$. The numbers in the graph indicate the values of k_1 and NL and L indicate the nonlinear and the linear case, respectively.

the continuous spectrum given by rapid distortion theory, whereas our result is obtained by forcing the boundary layer with one free-stream mode only.

The fact that LWG found good agreement between their low-frequency-band results and the experimental data by Kendall in the same frequency range (Figure 10 - page 192) could be due to the mild effect of nonlinearity at the downstream locations of comparison and to the low value of free-stream turbulence intensity. Our result is in qualitative agreement with the one presented by[31], who solved the *steady* nonlinear boundary-region equations forced by one free-stream mode. They found that nonlinearity is not influential at short downstream distances, but progressively brings about less intense fluctuations with respect to the linear case. This qualitative accordance seems to further indicate that the low-frequency streamwise disturbances behave in a quasi-steady manner during the early stage of the downstream evolution.[50] however remarked that unsteadyness is likely to play a critical role in the near-wall torsion of the Blasius profile, thereby enhancing the TS-breakdown mechanism.

The new mean flow U_M is as follow:

$$U_M = U_M(\overline{x}, \eta) = F'(\eta) + \hat{u}_{0,0}(\overline{x}, \eta).$$

We observe that the canonical Blasius profile is modified by the nonlinear interactions in that higher values of streamwise velocity are detected near the wall (increased wall-shear stress), whereas the opposite phenomenon occurs in the proximity of the free-stream (figure 9). This finding accords with the DNS calculations of[24] and[?] , who reported the existence of forward jets in the proximity of the wall and backward jets in the outer edge layer.

LWG also point out that the two-dimensional components, which are asymptotically smaller for isotropic free-stream turbulence in the linear case, might become important in the nonlinear case and interact with the three-dimensional ones.

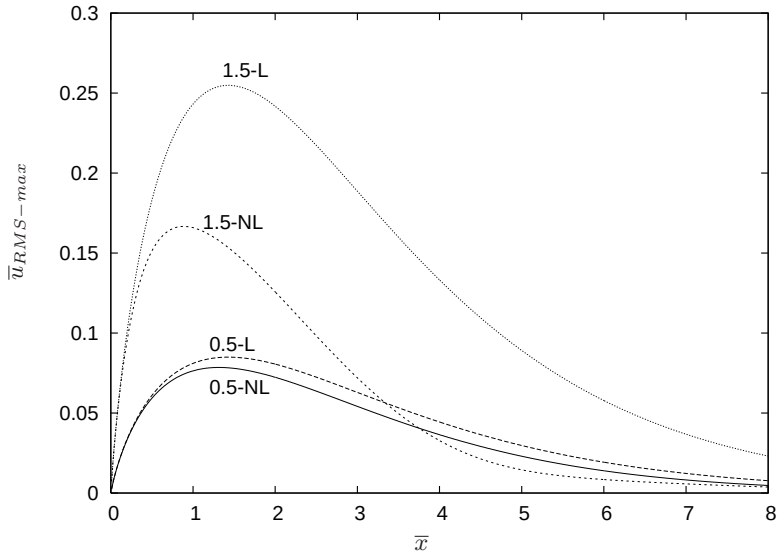

FIG. 8: Effect of variation of turbulence intensity on the maximum r.m.s. of the three-dimensional streamwise velocity for $\varepsilon = 0.01$, $k_1 = 0.01$, $k_2 = -k_3 = -1.0$ and $R_\Lambda = 400$. The numbers in the graph indicate the values of $\hat{u}^{\infty}_{1,2,3}$.

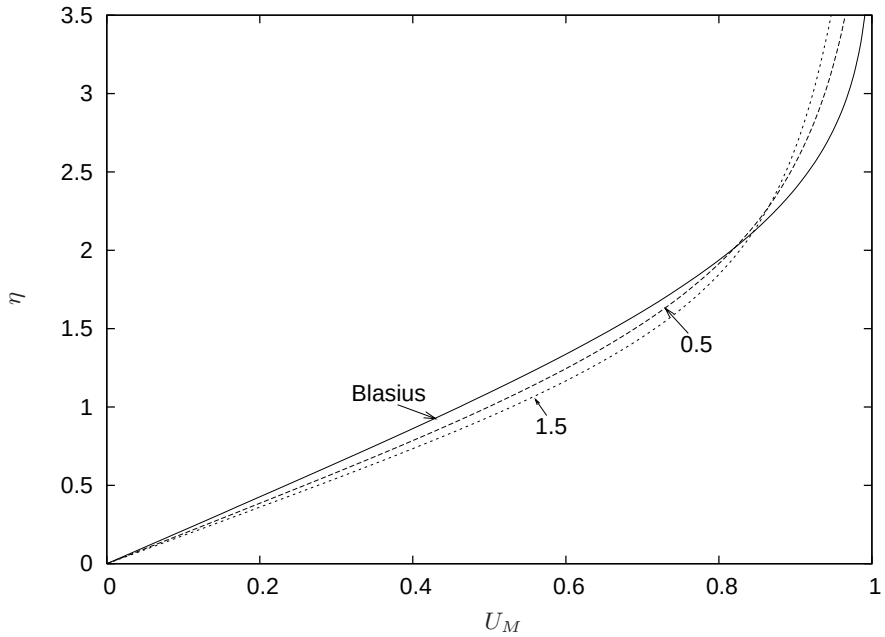

FIG. 9: Evolution of mean streamwise velocity profile at different downstream locations for $\varepsilon\hat{u}_{1,2,3} = 0.015, k_1 = 0.01$, $k_2 = -k_3 = -1.0$, and $R_\Lambda = 400$. Numbers in the graph denote the downstream location $\overline{x}$.

IV. FUTURE WORK

Future studies with multi-mode forcing in the free-stream are of interest, in particular the nonlinear interaction of two modes, one with low and the other one with high frequency. Recent results by[?] show that transition can occur with two modes of this kind. This finding is encouraging for our further research on bypass transition, since, as also envisioned by LWG, the nonlinear simulation with the continuous free-stream spectrum appears too computationally expensive at the present time. However, since the boundary-region formulation is accurate only for low values of k_1, it might not be possible to investigate the case with the high-frequency free-stream forcing.

It is also important to analyze the secondary instability of the new flow generated by the nonlinear interaction of the modes within the viscous region. This stability analysis has also been suggested by LWG. The purpose is to set a theoretical basis on the most prominent transition mechanism observed in the DNS simulations by[24], namely the Kelvin-Helmholtz type of instability of the lifted backward perturbation jets. This intriguing mechanism has been first recognized as relevant by[51] in their extensive work on bypass transition due to periodically passing wakes. These unstable phenomena eventually lead to the formation of "top-down" turbulent spots, so called since they are originated by a high-level of free-stream turbulence located *on top* of them. The merging of the spots then completes the transition to fully-developed turbulence.

It is also undoubtedly of interest to look for analogies with the recent results by[50] of a Blasius boundary layer perturbed by Klebanoff modes. They found that such free-stream perturbations can significantly distort the base mean flow to produce the inviscid growth of modified TS waves, which can be much higher than in the case of the unmodified Blasius flow. Furthermore, the analysis by[8] and the experiments by[3] indicate that moderate free-stream turbulence intensities are capable of generating a spatial amplification rate of disturbances which is lower than in the canonical case. However, they also observed that inflectional instability occurs for higher values of turbulence intensity, thereby enhancing the transition process. These peculiar behaviors deserve further investigation, which might lead us to a better understanding of the relation between the TS-wave breakdown and the lift-up mechanism of the laminar streaks. We however note that the new base flow for the secondary instability analysis should include the contribution of the streak modulation at fixed time. It should be possible to parametrize the effect of time on the streamwise velocity profile inasmuch as the laminar streaks evolve on a much longer time scale.

Acknowledgements

Pierre Ricco would like to acknowledge the hospitality and financial support of the Center for Turbulence Research at Stanford and to thank Professor S. Lele, Z. Xiong, Y. Liu for the useful and illuminating discussions. Part of PR's expenses during the Summer Research Program was covered by EPSRC grant GR/S59635/01.

REFERENCES

[1] P. Andersson, L. Brandt, A. Bottaro, and D. S. Henningson. On the breakdown of boundary layer streaks. *J. Fluid Mech.*, 428:29–60, 2001.

[2] D. Arnal and J. C. Juillen. Contribution expérimental a l'etude de la receptivite d'une couche limite laminaire, a la turbulence de l'ecoulement general. *CERT RT 1/5018 AYD - ONERA*, 1978.

[3] A. V. Boiko, K. J. A. Westin, K. G. B. Klingmann, V. V. Kozlov, and P. H. Alfredsson. Experiments in a boundary layer subjected to free stream turbulence. Part 2. The role of TS-waves in the transition process. *J. Fluid Mech.*, 281:219–245, 1994.
[4] K.M. Butler and B.F. Farrell. Three-dimensional optimal perturbations in viscous shear flow. *Phys. Fluids*, 4(8):1637–1650, 1992.
[5] C. Canuto, M.Y. Hussaini, A. Quarteroni, and T.A. Zang. *Spectral Methods in Fluid Dynamics*. Springer-Verlag, New York, 1988.
[6] P. Cathalifaud and P. Luchini. Algebraic growth in boundary layers: optimal control by blowing and suction at the wall. *Eur. J. Mech. - B Fluids*, 19:469–490, 2000.
[7] T. Cebeci. *Convective Heat Transfer*. Springer-Verlag, 2002.
[8] C. Cossu and L. Brandt. Stabilization of Tollmien-Schlichting waves by finite amplitude optimal streaks in the Blasius boundary layer. *Phys. Fluids*, 14(8):L57–L60, 2002.
[9] H. L. Dryden. Air flow in the boundary layer near a plate. *NACA Rep.*, 562, 1936.
[10] T. Ellingsen and E. Palm. Stability of linear flow. *Phys. Fluids*, 18(4):487–488, 1975.
[11] M. E. Goldstein. Unsteady vortical and entropic distortions of potential flows round arbitrary obstacles. *J. Fluid Mech.*, 89:433–468, 1978.
[12] M. E. Goldstein. The evolution of Tollmien-Schlichting waves near a leading edge. *J. Fluid Mech.*, 127:59–81, 1983.
[13] M. E. Goldstein. Generation of instability waves in flows separating from smooth surfaces. *J. Fluid Mech.*, 145:71–94, 1984.
[14] M. E. Goldstein. Scattering of acoustic waves into Tollmien-Schlichting waves by small streamwise variations in surface geometry. *J. Fluid Mech.*, 154:509–529, 1985.
[15] M. E. Goldstein. Response of the pre-transitional laminar boundary layer to free-stream turbulence - Otto Laporte Lecture. *Bull. Am. Phys. Soc.*, 42:2150, 1997.
[16] M. E. Goldstein and L. S. Hultgren. Boundary layer receptivity to long-wave free-stream disturbances. *Ann. Rev. Fluid Mech.*, 21:137–166, 1989.
[17] M. E. Goldstein and S. J. Leib. Three-dimensional boundary layer instability and separation induced by small-amplitude streamwise vorticity in the upstream flow. *J. Fluid Mech.*, 246:21–41, 1993.
[18] M. E. Goldstein, S. J. Leib, and S. J. Cowley. Distortion of a flat plate boundary layer by free stream vorticity normal to the plate. *J. Fluid Mech.*, 237:231–260, 1992.
[19] M. E. Goldstein and D. W. Wundrow. On the environmental realizability of algebraically growing disturbances and their relation to Klebanoff modes. *Theor. Comp. Fluid Dyn.*, 10:171–186, 1998.
[20] A. N. Gulyaev, V. E. Kozlov, V. R. Kuzenetsov, B. I. Mineev, and A. N. Sekundov. Interaction of a laminar boundary layer with external turbulence. *Fluid Dynamics. Translated from Izv, Akad. Navk. SSSR Mekh. Zhid. Gaza 6, vol. 5, pp. 55-65.*, 24(5):700–710, 1989.
[21] L.H. Gustavsson. Energy growth of three-dimensional disturbances in plane Poiseuille flow. *J. Fluid Mech.*, 224:241, 1991.
[22] L.S. Hultgren and L.H. Gustavson. Algebraic growth of disturbances in a laminar boundary layer. *Phys. Fluids*, 24(6):1000–1004, 1981.
[23] J. C. R. Hunt. A theory of turbulent flow round two-dimensional bluff bodies. *J. Fluid Mech.*, 61:625–706, 1973.
[24] R. G. Jacobs and P. A. Durbin. Simulation of bypass transition. *J. Fluid Mech.*, 428:185–212, 2001.
[25] N. Kemp. The laminar three-dimensional boundary layer and a study of the flow past a side edge. *MSc Thesis, Cornell University*, 1951.
[26] J. M. Kendall. Studies on laminar boundary layer receptivity to free-stream turbulence near a leading edge. *In Boundary Layer Stability and Transition to Turbulence (ed. D.C. Reda, H. L. Reed & R. Kobayashi). ASME FED*, 114:23–30, 1991.
[27] J. Kim, P. Moin, and R. Moser. Turbulence statistics in fully developed channel flow at low Reynolds number. *J. Fluid Mech.*, 177:133–166, 1987.
[28] P. S. Klebanoff. Effect of free-stream turbulence on a laminar boundary layer. *Bull. Am. Phys. Soc.*, 16:1323, 1971.
[29] M.T. Landahl. A note on an algebraic instability of inviscid parallel shear flows. *J. Fluid Mech.*, 98:243–251, 1980.
[30] S. J. Leib, D. W. Wundrow, and M. E. Goldstein. Effect of free-stream turbulence and other vortical disturbances on a laminar boundary layer. *J. Fluid Mech.*, 380:169–203, 1999.
[31] S. J. Leib, D. W. Wundrow, and M. E. Goldstein. Generation and growth of boundary-layer disturbances due to free-stream turbulence. *AIAA Paper 99-0498*, 1999.

[32] P. Luchini. Reducing the turbulent skin friction. In J.A. Desideri et al. – Wiley, editor, *Computational Methods in Applied Sciences – Proc. 3rd ECCOMAS CFD Conference*, pages 466 – 470, 1996.
[33] P. Luchini. Reynolds-number-independent instability of the boundary layer over a flat surface: optimal perturbations. *J. Fluid Mech.*, 404:289–309, 2000.
[34] P. Moin and K. Mahesh. Direct numerical simulation: a tool in turbulence research. *Annu. Rev. Fluid Mech.*, 30:539–578, 1998.
[35] M.V. Morkovin. Bypass transition to turbulence and research desiderata. *NASA CP-2386 Transition in Turbines*, pages 161–204, 1984.
[36] S. B. Pope. *Turbulent Flows*. Cambridge University Press, 2000.
[37] S.C. Reddy and D.S. Henningson. Energy growth in viscous channel flows. *J. Fluid Mech.*, 252:209–238, 1993.
[38] E. Reshotko. Boundary layer stability and transition. *Ann. Rev. Fluid Mech.*, 8:311–349, 1976.
[39] A. I. Ruban. On the generation of Tollmien-Schlichting waves by sound. *Fluid Dyn.*, 25(2):213–221, 1985.
[40] H. Schlichting. Zur Entstehung der Turbulenz bei der Plattenströmung. *Math. Phys. Klasse. Nach. Ges. Wiss. Göttingen*, pages 181–208, 1933.
[41] H. Schlichting and K. Gersten. *Boundary-Layer Theory*. Springer, 2000.
[42] G.B. Schubauer and H.K Skramstad. Laminar boundary-layer oscillations and transition on a flat plate. *NACA TN 909*, 1947.
[43] K.L Suder, J.E. O'Brien, and E. Reshotko. Experimental study of bypass transition in a boundary layer. *NASA TM 100913*, 1988.
[44] G. I. Taylor. Some recent developments in the study of turbulence. *Fifth Intl. Congr. for Appl. Mech. (ed. J.P. Den Hartog & Peters) - Wiley/Chapman and Hall, New York-London*, pages 294–310, 1939.
[45] W. Tollmien. Uber die Entstehung der Turbulenz 1. Mitteilung. in Math. Phys. Kl. (pp. 21–44). Nach. Ges. Wiss. Göttingen (Translated into English as NACA TM 609 (1931)). 1929.
[46] L.N. Trefethen, A.E. Trafethen, S.C. Reddy, and T.A. Driscoll. Hydrodynamic stability without eigenvalues. *Science*, 261:578–584, 1993.
[47] A. Tumin. A model of spatial algebraic growth in a boundary layer subjected to a streamwise pressure gradient. *Phys. Fluids*, 13(5):1521–1523, 2001.
[48] K. J. A. Westin, A. V. Boiko, B. G. B. Klingmann, V. V. Kozlov, and P. H. Alfredsson. Experiments in a boundary layer subjected to free stream turbulence. Part 1. Boundary layer structure and receptivity. *J. Fluid Mech.*, 281:193–218, 1994.
[49] X. Wu. Receptivity of boundary layers with distributed roughness to vortical and acoustic disturbances: A second-order asymptotic theory and comparison with experiments. *J. Fluid Mech.*, 431:91–133, 2001.
[50] X. Wu and M. Choudhari. Linear and non-linear instabilities of a Blasius boundary layer perturbed by streamwise vortices. Part 2. Intermittent instability induced by long-wavelength Klebanoff modes. *J. Fluid Mech.*, 483:249–286, 2003.
[51] X. Wu, R. G. Jacobs, J. C. R. Hunt, and P. A. Durbin. Simulation of boundary layer transition induced by periodically passing wakes. *J. Fluid Mech.*, 398:109–153, 1999.
[52] D. W. Wundrow and M. E. Goldstein. Effect on a laminar boundary layer of small-amplitude streamwise vorticity in the upstream flow. *J. Fluid Mech.*, 426:229–262, 2001.
[53] S. Zuccher, P. Luchini, and A. Bottaro. Algebraic growth in a Blasius boundary layer: optimal and robust control by mean suction in the nonlinear regime. *J. Fluid Mech.*, 513:135–160, 2004.